

Aspects of the Nonlinear Optical Properties as a Guide to Protonation Sites: A Theoretical Study upon α -Keggin $[\text{SiW}_{12}\text{O}_{40}]^{4-}$ and $[\text{SiV}_3\text{W}_9\text{O}_{40}]^{7-}$

Chan Yao,^{1,2} Chun-Guang Liu,^{1,2} Li-Kai Yan,^{1,2} Wei Guan,^{1,2} Ping Song,^{1,2} and Zhong-Min Su*^{1,2}

¹Institute of Functional Material Chemistry, Northeast Normal University, Changchun 130024, P. R. China

²Key Laboratory of Polyoxometalate Science of Ministry of Education, Faculty of Chemistry, Northeast Normal University, Changchun 130024, P. R. China

(Received February 12, 2010; CL-100146; E-mail: zmsu@nenu.edu.cn)

The present study focuses on probing the extent to which nonlinear optical effects act as a guide to protonation sites of α -Keggin heteropolyanions $[\text{SiW}_{12}\text{O}_{40}]^{4-}$ and $[\text{SiV}_3\text{W}_9\text{O}_{40}]^{7-}$. The second-harmonic generation (SHG) values of differently protonated forms predict that the molecular nonlinear optical activity has a close relationship with protonation sites and provides a new potential experimental probe.

Polyoxometalates (POMs) are a rich class of inorganic cluster systems and exhibit remarkable chemical and physical properties, which have been applied to a variety of fields, such as medicine, catalysis, biology, analytical chemistry, and materials science. The applications of POMs are often related to their ability to be protonated. During the past two decades, the locations of protons have been determined by nuclear magnetic resonance (NMR) measurements, spectroscopic measurements, and density functional theory (DFT) calculations, and large amount of work focuses on the most common and thermally stable Keggin structure.^{1–8} Despite this, the results remain ambiguous. More recently, some experiments and theoretical investigations reveal that the protonation strongly affects the molecular second-order polarizability,^{9–11} and the nonlinear optical (NLO) properties of Keggin POMs have been reported based on many experiments and theories.^{12,13} Herein, the extent to which nonlinear optical effects act as a guide to protonation sites of α -Keggin POMs is explored.

DFT calculations were carried out using the ADF program.¹⁴ Geometry optimizations have been carried out using the BP86^{15,16} density functional approach with triple- ξ -plus-polarization quality (TZP) Slater orbital basis sets and incorporating frozen cores (O 1s, Si 2p, W 4d, and V 3p) and ZORA relativistic correction.^{17,18} Time-dependent density functional theory (TDDFT) calculations were pursued using the asymptotically correct functional of van Leeuwen and Baerends (LB94).¹⁹ The linear response equation of TDDFT was adopted to compute linear polarizability, α , and the $(2n + 1)$ theorem was used for obtaining the second-order polarizability β . The α -Keggin $[\text{SiW}_{12}\text{O}_{40}]^{4-}$ and trisubstituted $[\text{SiV}_3\text{W}_9\text{O}_{40}]^{7-}$ are chosen, and the structures are identified in Figure 1. There are four types of oxygen atoms in $[\text{SiW}_{12}\text{O}_{40}]^{4-}$: four in the central tetrahedron (O_a), twelve that bridge two W atoms sharing the same central oxygen atom (edge-sharing, O_b), twelve that bridge two W atoms not sharing the same central oxygen atom (corner-sharing, O_c), and twelve terminal oxygen atoms (O_d) associated with a single W atom. The systems with protonated positions at O_b , O_c , and O_d are expressed as IO_b , IO_c , and IO_d in set I. There are nine types of oxygen atoms in $[\text{SiV}_3\text{W}_9\text{O}_{40}]^{7-}$ except four oxygen atoms (O_a) in the central tetrahedron: three types of oxygen

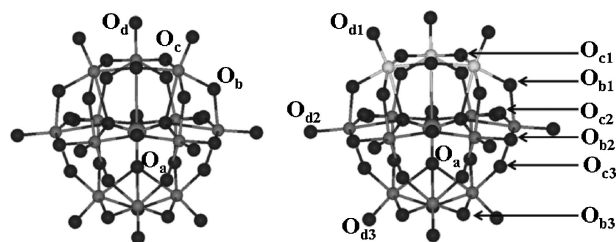


Figure 1. The Keggin structures of $[\text{SiW}_{12}\text{O}_{40}]^{4-}$ and $[\text{SiV}_3\text{W}_9\text{O}_{40}]^{7-}$, identifying the all types of oxygen atoms.

atoms bridge two metal atoms sharing the same central oxygen atom (O_{b1} ($\text{V}-\text{O}-\text{W}_{\text{belt}}$), O_{b2} ($\text{W}_{\text{belt}}-\text{O}-\text{W}_{\text{belt}}$), and O_{b3} ($\text{W}_{\text{cap}}-\text{O}-\text{W}_{\text{cap}}$)), three types of oxygen atoms bridge two metal atoms not sharing the same central oxygen atom (O_{c1} ($\text{V}-\text{O}-\text{V}$), O_{c2} ($\text{W}_{\text{belt}}-\text{O}-\text{W}_{\text{belt}}$), and O_{c3} ($\text{W}_{\text{belt}}-\text{O}-\text{W}_{\text{cap}}$)), and three types of terminal oxygen atoms (O_{d1} ($\text{V}-\text{O}$), O_{d2} ($\text{W}_{\text{belt}}-\text{O}$), and O_{d3} ($\text{W}_{\text{cap}}-\text{O}$)). The systems with protonated positions at the nine types of oxygen atoms are expressed as HIO_{b1} , HIO_{b2} , HIO_{b3} , HIO_{c1} , HIO_{c2} , HIO_{c3} , HIO_{d1} , HIO_{d2} , and HIO_{d3} in set II.

In view of generality, all of the possible protonated models were investigated. This is different from the previous computational studies based on proton affinity and molecular electrostatic potential.^{6–8} The proton on each type of oxygen has several orientations including toward and away from the M_3O_3 ($\text{M} = \text{W}$ or V) ring. Much computation is required to determine the orientation of protons on each type of oxygen atom, especially for possible protonated models of $[\text{SiV}_3\text{W}_9\text{O}_{40}]^{7-}$ which has nine types of oxygen atoms. Protonation removes all symmetry elements and the calculations are performed without symmetry restrictions. The relative energies (in kcal mol^{-1}) are listed in Table S1 (see Supporting Information).²⁰ The most stable protonation state in set I is IO_c in which the proton is attached to O_c . The next preferred site is O_b with a relative energy of only $2.6 \text{ kcal mol}^{-1}$. O_d is the least stable site and IO_d lies at 15 kcal mol^{-1} . The difference in the proton affinity between the most and least basic sites being ca. 15 kcal mol^{-1} in set I. In set II, the HIO_{c1} is the most stable isomer, and the stability decreases in the following order: $\text{HIO}_{c1} > \text{HIO}_{b1} > \text{HIO}_{c2} > \text{HIO}_{b2} > \text{HIO}_{c3} > \text{HIO}_{b3} > \text{HIO}_{d1} > \text{HIO}_{d2} > \text{HIO}_{d3}$. The difference between HIO_{c1} and HIO_{d3} is ca. 30 kcal mol^{-1} , which is ca. 15 kcal mol^{-1} larger than that of set I. It can be concluded that the substitution by three V atoms affects the relative basicity and nucleophilicity of the substituted region.

A measurement of the second-order polarizability $\beta(-2\omega; \omega, \omega)$ is related to second-harmonic generation (SHG). Based on the optimized structures, TDDFT calculations were carried out to investigate the second-order polarizabilities of the protonation

Table 1. The second-order polarizabilities at $\omega = 0.0$ eV (β_0^{Static}) and $\omega = 0.65$ eV (β_0^{SHG}) for studied systems in set I and II (au)

	β_0^{Static}	β_0^{SHG}
IO_b	263.8	318.7
IO_c	247.3	293.8
IO_d	214.7	226.2
IIO_{b1}	810.4	1189.7
IIO_{b2}	991.3	1396.2
IIO_{b3}	1131.9	1572.9
IIO_{c1}	509.4	718.8
IIO_{c2}	698.6	1016.7
IIO_{c3}	1040.1	1470.3
IIO_{d1}	313.2	418.3
IIO_{d2}	599.3	758.2
IIO_{d3}	985.0	1328.7

states in sets **I** and **II**. The second-order polarizabilities calculated under the static electronic field and the laser frequency of $\omega = 0.65$ eV ($\lambda = 1907$ nm) are listed in Table 1. It can be seen that the SHG values are larger than the static values for all the systems and present an enlarged discrepancy between each other. The smallest discrepancy in set **I** is about 25 au, found between systems **IO_b** and **IO_c**. The SHG values decrease as the protonation site changes in the order $O_b > O_c > O_d$. The SHG value of system **IIO_{b3}** is 1572.9 au, which is four times larger than that of system **IIO_{d1}** (418.3 au), and the discrepancy between them is the largest in set **II**. The smallest discrepancy is found between systems **IIO_{c1}** and **IIO_{d2}**, which is about 40 au. For the proton location of the same type of oxygen atoms, the SHG values increase in the order $1 < 2 < 3$ (**IIO_{b1}** < **IIO_{b2}** < **IIO_{b3}**, **IIO_{c1}** < **IIO_{c2}** < **IIO_{c3}**, and **IIO_{d1}** < **IIO_{d2}** < **IIO_{d3}**), and for the proton location of different types of oxygen atoms, the SHG values decrease in the order $b > c > d$ (**IIO_{b1}** > **IIO_{c1}** > **IIO_{d1}**, **IIO_{b2}** > **IIO_{c2}** > **IIO_{d2}**, and **IIO_{b3}** > **IIO_{c3}** > **IIO_{d3}**). Namely, the systems with the protonation site away from vanadium atoms generate larger SHG values than the systems with the protonation site near vanadium atoms, and the systems with protonation site at the bridging oxygen atoms appear to generate larger SHG values than the systems with the protonation site at terminal oxygen atoms. To understand the position effect of proton on the NLO response, the two-level model of second-order polarizability is considered (see Supporting Information).²⁰ It is obvious that the great influence on the transition energy, which is a decisive factor to determine the NLO response, is provided by position effects of protons. Thus, different protonation sites cause significant changes in the second-order NLO activity. From these results, it can be concluded that protonation sites can probe SHG values indirectly.

In summary, the relationship between the protonation sites

and NLO properties of α -Keggin structures $[\text{SiW}_{12}\text{O}_{40}]^{4-}$ and $[\text{SiV}_3\text{W}_9\text{O}_{40}]^{7-}$ has been studied by TDDFT calculation for the first time. The SHG values under the optical frequency ($\hbar\omega = 0.65$ eV) predict that the NLO activities of the title models are intimately associated with protonation sites, and the second-order polarizability can be a guide to the localization of proton. It is hoped that the results presented in this paper will provide a new way to determine the protonation sites for experimentalists.

References and Notes

- I. V. Kozhevnikov, A. Sinnema, H. Bekkum, *Catal. Lett.* **1995**, *34*, 213.
- S. Ganapathy, M. Fournier, J. F. Paul, L. Delevoye, M. Guelton, J. P. Amoureux, *J. Am. Chem. Soc.* **2002**, *124*, 7821.
- K. Y. Lee, N. Mizuno, T. Okuhara, M. Misono, *Bull. Chem. Soc. Jpn.* **1989**, *62*, 1731.
- J. B. Moffat, *J. Mol. Catal.* **1984**, *26*, 385.
- T. Ueda, T. Tatsumi, T. Eguchi, N. Nakamura, *J. Phys. Chem. B* **2001**, *105*, 5391.
- M. J. Janik, K. A. Campbell, B. B. Bardin, R. J. Davis, M. Neurock, *Appl. Catal., A* **2003**, *256*, 51.
- J. Yang, M. J. Janik, D. Ma, A. Zheng, M. Zhang, M. Neurock, R. J. Davis, C. Ye, F. Deng, *J. Am. Chem. Soc.* **2005**, *127*, 18274.
- X. López, C. Bo, J. M. Poblet, *J. Am. Chem. Soc.* **2002**, *124*, 12574.
- C. C. Evans, M. Bagieu-Beucher, R. Masse, J. Nicoud, *Chem. Mater.* **1998**, *10*, 847.
- P. G. Lacroix, C. Lepetit, J. C. Daran, *New J. Chem.* **2001**, *25*, 451.
- I. Asselberghs, G. Hennrich, K. Clays, *J. Phys. Chem. A* **2006**, *110*, 6271.
- H. Murakami, T. Kozeki, Y. Suzuki, S. Ono, H. Ohtake, N. Sarukura, E. Ishikawa, T. Yamase, *Appl. Phys. Lett.* **2001**, *79*, 3564.
- Y.-M. Xie, Q.-S. Zhang, Z.-G. Zhao, X.-Y. Wu, S.-C. Chen, C.-Z. Lu, *Inorg. Chem.* **2008**, *47*, 8086.
- ADF: Amsterdam Density Functional Software 2008*, Department of Theoretical Chemistry, Vrije Universiteit, Amsterdam, The Netherlands, **2008**.
- A. D. Becke, *Phys. Rev. A* **1988**, *38*, 3098.
- J. P. Perdew, *Phys. Rev. B* **1986**, *33*, 8822.
- E. van Lenthe, E. J. Baerends, J. G. Snijders, *J. Chem. Phys.* **1993**, *99*, 4597.
- E. van Lenthe, A. E. Ehlers, E.-J. Baerends, *J. Chem. Phys.* **1999**, *110*, 8943.
- R. van Leeuwen, E. J. Baerends, *Phys. Rev. A* **1994**, *49*, 2421.
- Supporting Information is available electronically on the CSJ-Journal Web site, <http://www.csj.jp/journals/chem-lett/index.html>.